Available online at www.sciencedirect.com

ScienceDirect

Journal of Otology 11 (2016) 118–126

www.journals.elsevier.com/journal-of-otology/

Trimethyltin-induced cochlear degeneration in rat

Jintao Yu [a,b,d], Dalian Ding [b,d,*], Hong Sun [d], Richard Salvi [b], Jerome A. Roth [c]

[a] Department of Otolaryngology, Union Hospital, Tongji Medical College, Huazhong University of Science and Technology, Wuhan 430022, China
[b] Center for Hearing and Deafness, University at Buffalo, Buffalo, NY 14214, USA
[c] Department of Pharmacology and Toxicology, University at Buffalo, Buffalo, NY 14214, USA
[d] Department of Otolaryngology Head and Neck Surgery, Xiangya Hospital, Central South University, Changsha, Hunan 410008, China

Received 20 June 2016; revised 27 July 2016; accepted 29 July 2016

Abstract

Trimethyltin (TMT) is an occupational and environmental health hazard behaving as a potent neurotoxin known to affect the central nervous system as well as the peripheral auditory system. However, the mechanisms underlying TMT-induced ototoxicity are poorly understood. To elucidate the effects of TMT on the cochlea, a single injection of 4 or 8 mg/kg TMT was administered intraperitoneally to adult rats. The compound action potential (CAP) threshold was used to assess the functional status of the cochlea and histological techniques were used to assess the condition of the hair cells and auditory nerve fibers. TMT at 4 mg/kg produced a temporary CAP threshold elevation of 25–60 dB that recovered by 28 d post-treatment. Although there was no hair cell loss with the 4 mg/kg dose, there was a noticeable loss of auditory nerve fibers particularly beneath the inner hair cells. TMT at 8 mg/kg produced a large permanent CAP threshold shift that was greatest at the high frequencies. The CAP threshold shift was associated with the loss of outer hair cells and inner hair cells in the basal, high-frequency region of the cochlea, considerable loss of auditory nerve fibers and a significant loss of spiral ganglion neurons in the basal turn. Spiral ganglion neurons showed evidence of soma shrinkage and nuclear condensation and fragmentation, morphological features of apoptotic cell death. TMT-induced damage was greatest in the high-frequency, basal region of the cochlea and the nerve fibers beneath the inner hair cells were the most vulnerable structures.

Keywords: Trimethyltin; Ototoxicity; Hair cells; Nerve fibers; Spiral ganglion neurons

1. Introduction

Chronic exposure to heavy metals and their organic derivatives can cause serious and potentially lethal harm to humans (Jarup, 2003; Prasher, 2009). Many heavy metals such as lead, mercury, cadmium, arsenic, manganese, cobalt, platinum and copper, which are widely used in manufacturing, are neurotoxic leading to a diverse array of debilitating clinical symptoms (Ding et al., 1999, 2007, 2009, 2011a, b, c; Bencko et al., 2009; Ikeda et al., 2010; He et al., 2011; Li et al., 2011; Shargorodsky et al., 2011; Wu et al., 2011; Ding et al., 2012a, Ding et al., 2012b; Hoshino et al., 2012; Ding et al., 2013; Liu et al., 2014; Wang et al., 2014; Li et al., 2015). During manufacturing, many heavy metals are inadvertently released into the environment posing serious risk to the public. Trimethyltin (TMT) is a short-chain organotin compound, notable for its deleterious effects on the central nervous system (CNS) (Koczyk, 1996). In experimental animals, TMT exposure selectively induces neuronal loss in the limbic system, including the hippocampus, pyriform cortex, olfactory tubercle, amygdala, and neocortex (Geloso et al., 2011). Rats exposed to TMT by intraperitoneal injection, develop a syndrome characterized by seizures, tail mutilation, vocalizations, hyperactivity, aggression, hearing loss and learning

* Corresponding author. Center for Hearing and Deafness, State University at Buffalo, Buffalo, NY 14214, USA. Fax: +1 716 829 2980.
E-mail address: dding@buffalo.edu (D. Ding).
Peer review under responsibility of PLA General Hospital Department of Otolaryngology Head and Neck Surgery.

http://dx.doi.org/10.1016/j.joto.2016.07.001

impairment, all of which represent the classic symptoms of which are known as the "TMT syndrome" (Dyer et al., 1982; Clerici et al., 1991). Human TMT exposure, which typically occurs by inhalation, produces a similar malady with disorientation, amnesia, aggressive behavior, ataxia, complex partial seizures and hearing loss (Besser et al., 1987). TMT induced neurobehavioral and neuropathological symptoms are similar in some respects to other neurodegenerative disorders such as Alzheimer's disease (AD) and temporal lobe epilepsy (TLE) (Ishikura et al., 2002; Nilsberth et al., 2002). Accordingly, TMT, frequently administered by intraperitoneal injection, is often used as a tool for studying neuronal degeneration that is associated with cognitive impairment and seizures (Besser et al., 1987; Clerici et al., 1991; Geloso et al., 2011).

In addition to the neurotoxic effects in CNS, TMT is highly ototoxic, producing hearing impairment even at very low doses of exposure (Fechter and Liu, 1995). For example, a single intraperitoneal injection of 2 mg/kg of TMT in guinea pigs resulted in impaired hearing thresholds within 30 min of administration (Clerici et al., 1991). The mechanisms underlying TMT-induced ototoxicity remain poorly understood. TMT appears to directly damage the cochlea (Fechter et al., 1986) reducing the cochlear microphonic (CM) amplitude, which largely reflects the electromechanical response of outer hair cells (OHC) as well as the compound action potential (CAP), a neural response from the auditory nerve initiated at the inner hair cells (IHC) and relayed across the afferent synapse to the spiral ganglion neurons (SGN). These results suggest that TMT could damage the OHC, IHC, the afferent synapse and SGN (Clerici et al., 1991; Fechter et al., 1992). However, the specific anatomical targets of TMT-induced cochlear damage are still poorly understood. Recent in vitro studies in our laboratory demonstrated that TMT preferentially damages SGN and their peripheral afferent nerve fibers with surprisingly little impact on the sensory hair cells in rat cochlear organotypic cultures (Yu et al., 2015). These results suggest that the SGN and auditory nerve fibers may be the most susceptible to TMT-induced damage. To better understand the mechanisms and *in vivo* cellular targets responsible for TMT ototoxicity, rats were treated with 4 or 8 mg/kg of TMT. The CAP was used to characterize the time course and frequency-specific nature of the hearing impairment and their cochleae harvested to determine the magnitude and location of hair cell loss and damage to the auditory nerve fibers and spiral ganglion neurons.

2. Materials and methods

2.1. Animal treatment

Female Sprague–Dawley rats weighing between 250 and 350 g were used for this study. All animal procedures were approved by the institutional animal care and use committee of the Xiangya Hospital, Central South University. Thirty-two animals with normal hearing were randomly divided into three groups: control group (n = 8), TMT 4 mg/kg treatment group (n = 12), and TMT 8 mg/kg treatment group (n = 12). These doses we employed were somewhat higher than those in the guinea pig, because rats tend to be less susceptible to ototoxicants than guinea pig. Some rats were exclusive used for anatomical studies while others were used for both histological analysis and CAP recordings. Rats in the two TMT-treated groups received a single intraperitoneal (i.p.) injection of TMT at either 4.0 mg/kg or 8.0 mg/kg body weight. TMT was dissolved in 1.0 ml normal saline (concentration 4 or 8 mg/ml). Rats in control group received a single injection (i.p.) of saline vehicle. Cochlear auditory function and histopathologies were examined at various time intervals after TMT treatment.

2.2. CAP

To evaluate the changes in the CAP versus time after TMT injection, a silver electrode was implanted into the facial nerve canal via the stylomastoid foramen. Our surgical approach for electrode implantation and procedure for CAP recording have been described previously (Yu et al., 2014). Ophthalmic ointment (Puralube Vet ointment, Dechra Veterinary Product) was put on the cornea daily to prevent visual impairment caused by facial paralysis after electrode implantation in facial nerve canal. During CAP testing, rats were anesthetized with a mixture of ketamine (50 mg/kg i.p.) and xylazine (6 mg/kg, i.p.). Body temperature was maintained at 37 °C using a heating pad. The CAP was recorded using TDT system III equipment (Tucker–Davis Technologies, USA). Tone burst stimuli at 4, 8, 16 and 32 kHz were digitally synthesized with a 3 ms duration and 0.5 ms rise-fall time and delivered at 21 times/s. Evoked potentials were filtered between 100 and 3000 Hz, and averaged 100 times. Thresholds were obtained by reducing the sound intensity in 5 dB increments from 90 dB SPL until the response completely disappeared. The lowest sound level that elicited a reproducible N1 wave in the CAP was defined as threshold. The amplitude of CAP stimulated by tone burst at 4, 8, 16, 32 kHz at 80 dB (SPL) was measured. The value of CAP from baseline to the peak of N1 wave was defined as CAP amplitude. The latency of CAP stimulated by tone burst at 4, 8, 16, 32 kHz was also measured. The time from the onset of sound stimulus by 80 dB (SPL) tone burst to the onset of the CAP was defined as CAP latency.

2.3. Cochlear hair cell staining and quantifications

Immediately after completing the functional tests, the anesthetized rat was decapitated. The cochleae were rapidly removed and the oval and round windows and the apex opened. The cochleae were perfused with a solution of succinate dehydrogenase (SDH, 2.5 ml of 0.2 M sodium succinate, 2.5 ml of 0.2 M phosphate buffer, pH 7.6, and 5 ml of 0.1% tetranitro blue tetrazolium) and subsequently immersed in the solution at 37 °C for 45 min. Afterwards, the cochleae were fixed in 10% formalin in PBS overnight. Under dissection microscope, the cochlear basilar membrane was carefully dissected out and specimens were mounted on glass slides and coverslipped. Hair cell counting was performed under a light

microscope and individual cochleograms were constructed for each ear by plotting the percent hair cell loss as a function of percent distance from the apex of the cochlea. Individual cochleograms were aggregated to generate a mean cochleogram for each group using custom software.

2.4. Immunostaining and histology

For immunostaining, animals were anesthetized and perfused transcardially with 10% formalin solution. Cochleae were removed and fixed in the same fixative at 4 °C for 2 h. After rinsing in PBS, the whole basilar membrane containing SGNs were dissected out and immersed in 10% goat serum and 0.2%Trition X-100 in PBS for 2 h. The samples were incubated overnight at 4 °C with a monoclonal primary mouse anti-neurofilament 200 antibody (Sigma, N0142) diluted in PBS containing 1% Triton X-100 and 5% goat serum (1:100). The following day specimens were rinsed three times with PBS and incubated in a secondary goat anti-mouse antibody conjugated with Alexa Fluor488 (Life technologies, A11001) diluted in PBS (1:200) for 2 h. Specimens were subsequently treated with the nuclear stain, To-Pro-3, (Life technologies, T3605) for 30 min. Tissues were then mounted on glass slides in glycerin, coverslipped, and examined under a confocal microscope (Zeiss LSM-510).

For sectioning, cochleae were removed as above and fixed in 2.5% glutaraldehyde overnight at 4 °C. After decalcification with 3% hydrochloric acid and further post-fixation in 1% osmium, the cochleae were dehydrated through a gradient alcohol and acetone series and embedded in Epon 812. The cochleae were sectioned serially at a thickness of 4 μm parallel to the cochlear modiolus as described previously (Wang et al., 2003). Sections were collected on glass slides, stained with toluidine blue, examined and photographed under a light microscope. The density of SGN was quantified using image J software as previously described (Yu et al., 2014). The boundary of the Rosenthal's canal was outlined and its cross-sectional area was measured by image J software. The numbers of SGN in Rosenthal's canal were counted and the density of SGN was obtained by dividing the number of SGN by the area of the area of Rosenthal's canal.

2.5. Statistical analysis

Statistical analyses were performed with GraphPad Prism software (version 5) as described below with the significance level set at $p < 0.05$.

3. Results

3.1. CAP changes post-TMT

To evaluate the effect of TMT on cochlear function, the CAP was recorded with the facial nerve canal electrode before and then 30 min, 1, 7, 14, 21 and 28 days post-TMT exposure. In the control group, CAP threshold did not change significantly compared to pre-treatment values at any time point (data not shown). However, significant changes in thresholds, amplitudes, and latencies of CAP were observed after the 4 and 8 mg/kg TMT treatments (Fig. 1). Mean (+/− SEM) CAP thresholds in 4 ($n = 5$) and 8 mg/kg ($n = 6$) TMT groups were significantly elevated at 30 min post-TMT and continued to increase out to 1 or 7 days post-TMT depending on dose and frequency. At 7 d post-TMT, CAP threshold shifts in 4 mg/kg group were about 60, 25, 25 and 20 dB at 32, 16, 8 and 4 kHz respectively (Fig. 1A), but then declined at longer recovery time so that CAP thresholds were back to near normal at 28 d post-TMT. At 7 d post-TMT, CAP threshold shifts in the 8 mg/kg group were roughly 65, 40, 45 and 30 dB at 32, 16, 8 and 4 kHz respectively (Fig. 1B). Threshold declined slightly between 7 and 14 d post-TMT and then either remained stable or increased slightly out to 28 d post-TMT resulting permanent CAP threshold shifts of approximately 60, 40, 25 and 20 dB at 32, 16, 8 and 4 kHz respectively.

A two-way repeated measures analysis of variance with Bonferroni posttests were carried out on the CAP data focusing on the change in threshold relative to baseline. For the 4 mg/kg group there were significant main effects of frequency ($F = 56.7$; 3, 96 DF; $p<<0.001$), time ($F = 51.3$; 6, 96 DF; $p < 0.001$) and the interaction of frequency and time ($F = 2.06$; 18, 96 DF; $p < 0.0001$). CAP threshold at 4 kHz were significantly higher than baseline from 1 to 14 d post-treatment ($p < 0.05$) but were back to normal at 21 and 28 d. Thresholds at 8 kHz were higher than normal between 30 min and 14 d post-treatment ($p < 0.05$), but were essentially normal at 21 and 28 d post-treatment. Thresholds at 16 kHz and 32 kHz were significantly ($p < 0.05$) above baseline between 30 min and 21 d post-treatment but were within normal limits at 28 d post-treatment. In the 8 mg/kg TMT group, there were significant main effects for frequency ($F = 103.3$; 6, 120 DF; $p < 0.0001$), time ($F = 64.2$; 3, 12 DF; $p < 0.0001$) and frequency−time interaction ($F = 4.1$; 20 120 DF; $p < 0001$). CAP thresholds at 4, 8, 16 and 32 kHz were significantly higher than baseline from 30 min to 28 d post-treatment.

In comparison with pre-testing, mean (+/− SEM) CAP amplitudes at 32, 16, 8, and 4 kHz measured at 80 dB (SPL) in both 4 mg/kg ($n = 5$) and 8 mg/kg ($n = 6$). TMT groups were significantly decreased 28 days post-TMT (Fig. 1C, D). Mean (+/− SEM) CAP latencies at 32, 16, 8, and 4 kHz at 80 dB (SPL) did not changed significantly in 4 mg/kg TMT group (Fig. 1E) 28 days post-TMT. However, the CAP latencies at all frequencies were significantly delayed 28 days post-treatment in the 8 mg/kg TMT group (Fig. 1F).

3.2. Hair cell loss

To determine if TMT damaged hair cell, OHC and IHC losses were evaluated 7 days post-TMT. Representative photomicrographs of SDH-stained surface preparations are shown in Fig. 2A. In control cochleae the IHC and OHC were intensely stained with SDH in the apical, middle and basal turn of the cochlea. A similar pattern of SDH labeling was observed in OHC and IHC in the 4 mg/kg TMT group.

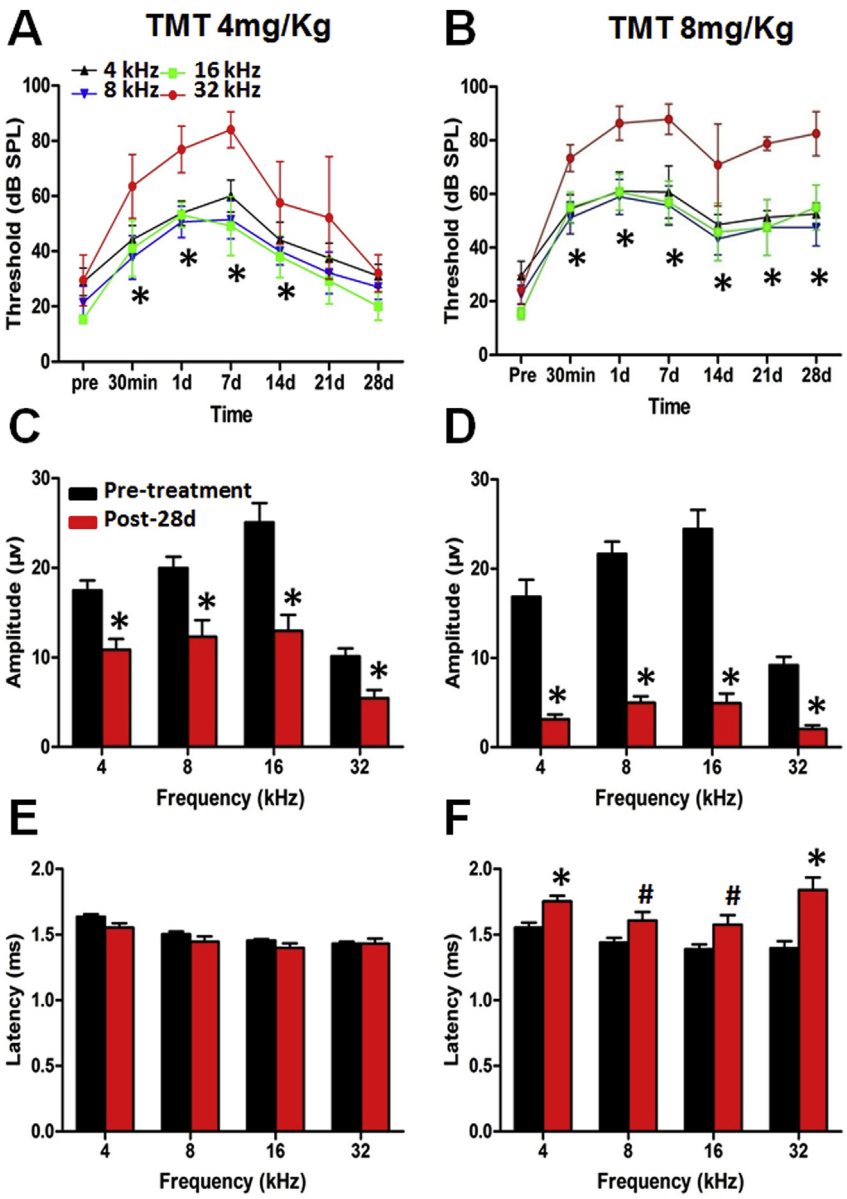

Fig. 1. Changes in thresholds, amplitudes, and latencies of CAP before and after TMT treatment. A,B: Mean (+/− SEM) CAP thresholds before, and 30 min, 1, 7, 14, 21, and 28 days following 4 mg/kg TMT treatment (n = 5), or 8 mg/kg TMT treatment (n = 6). C,D: Mean (+/− SEM) CAP amplitude before, and 30 min, 1, 7, 14, 21, and 28 days following 4 mg/kg TMT treatment (n = 5), or 8 mg/kg TMT treatment (n = 6). E,F: Mean (+/− SEM) CAP latencies before, and 30 min, 1, 7, 14, 21, and 28 days following 4 mg/kg TMT treatment (n = 5), or 8 mg/kg TMT treatment (n = 6).

However, in the 8 mg/kg TMT group, SDH staining was absent from almost all OHC as well as some IHC in the basal turn. However, SDH labeling was present in most OHC and IHC in the apical and middle turn. Mean (n = 5) cochleograms showing the percent missing OHC and IHC for the control group and the 4 and 8 mg/kg TMT group are shown in Fig. 2B. Average hair cell loss was less than 5% along the entire length of the cochlea in the control group as well as in the 4 mg/kg TMT group. In the 8 mg/kg TMT group, the mean OHC loss decreased from about 60% at the 90% location to less than 10% loss at the 60% location. The mean IHC loss was restricted to the extreme base and decreased from approximately 50% at the 90% location to less than 10% loss at the 80% location.

3.3. Cochlear nerve fiber damage

To assess the effects of TMT on cochlear nerve terminals, we immunostained the cochlea with an antibody against neurofilament 200 kDa to reveal the peripheral nerve fibers in the sensory epithelium. Fig. 4 illustrates the typical status of cochlear nerve fibers in control and TMT-treated groups seven days post-treatment. In controls, the nerve fibers exit the habenula perforata and project out to the organ of Corti in a well-organized pattern. Many nerve fibers end in the vicinity of the IHC mostly near the basal pole. Based on the location of neurofilament immunolabeling, the majority of these are presumably type I afferent auditory nerve fibers that comprise 90–95% of all afferents (Spoendlin, 1978), but some may be

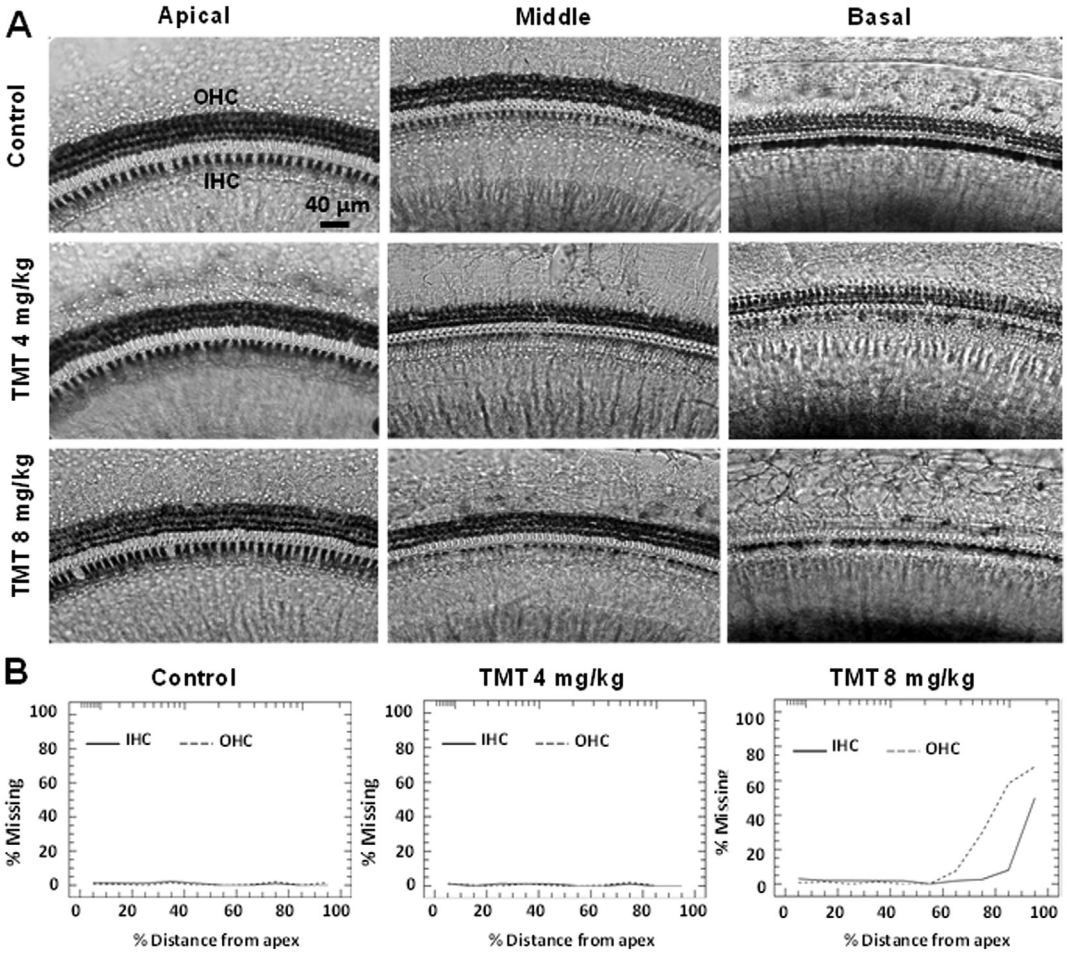

Fig. 2. Hair cell loss after TMT treatment. (A) Representative photomicrographs (200X) of surface preparation from the apical, middle and basal turn of the cochlea from the control group and 4 mg/kg and 8 mg/kg TMT groups 7 days post-treatment. Samples labeled with succinate dehydrogenase which intensely stains the outer hair cells (OHC) and inner hair cells (IHC). Note significant loss of staining of OHC and IHC in the basal turn of the 8 mg/kg TMT group. (B) Mean cochleograms (n = 5/group) from the control group and the 4 and 8 mg/kg TMT groups. Cochleograms show the percent missing IHC and OHC as a function of percent distance from the apex of the cochlea.

medial olivocochlear efferent fibers (Fig. 3A, a) (White and Warr, 1983). A minority of the neurofilament-labeled fibers crossing the tunnel of Corti and projecting to the three rows of OHC are likely the medial olivocochlear efferent fibers and the afferent processes of type II SGN (White and Warr, 1983; Warr, 1992). In the 4 mg/kg TMT group, there were far fewer neurofilament-labeled fibers in the IHC region and a reduction in the number of fibers projecting to the OHC (Fig. 3B, b). Some fibers in the 4 mg/kg TMT group were distorted and looped in the tunnel of Corti rather than projecting radially (arrowhead, Fig. 3B). In the 8 mg/kg TMT group, there was a further reduction in the number of fibers in IHC region and those projecting to the OHC region (Fig. 3C, c). Since most OHCs were missing, some nerve fibers looped around and crossed over one another (asterisk). .

3.4. Spiral ganglion neuron degeneration

The survival of SGN was evaluated seven days after TMT treatment from plastic embedded cross sections of the Rosenthal's canal. Fig. 4A–C displays representative micrographs of the SGN in Rosenthal's canal for the lower basal turn of the cochlea from a representative control animal and animals from the 4 and 8 mg/kg TMT-groups. In the control group, Rosenthal's canal was densely packed with SGNs and thick fascicles of fibers (Fig 4A). In the 4 mg/kg TMT-group, the number and the condition of the SGNs and auditory nerve fibers (ANFs) appeared similar to the controls (Fig. 4B). In contrast, severe loss of SGNs and ANFs was evident in the lower basal turn of the cochlea in the 8 mg/kg TMT group, particularly in the hook region. However, there was no evidence of damage to SGN and ANFs in more apical regions of the cochlea (data not shown). To quantify the results, SGN counts were performed in the hook region of 5 control rats, 5 rats in 4 mg/kg TMT group and 6 rats in the 8 mg/kg TMT group. SGN counts were measured with an area of 0.0144 mm^2 at three locations within the hook region and mean value computed for each rat. To compare the results, the SGN density measures rats in the TMT group were normalized to the control and expressed as a percentage of the controls. As

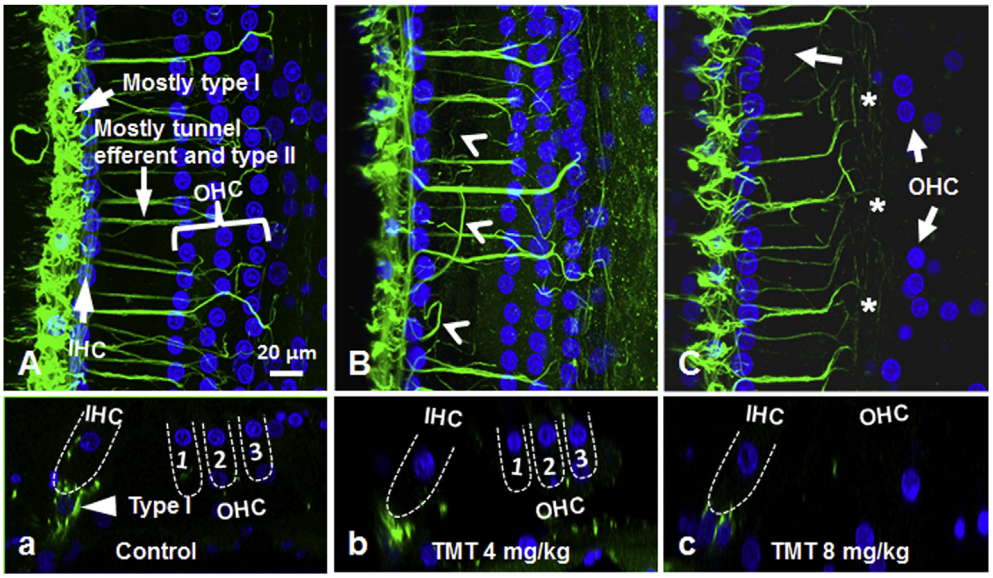

Fig. 3. Representative confocal images showing the condition of cochlear nerve fibers from the basal turn of the cochlea 7 d post-treatment. Nerve fibers labeled with antibody against neurofilament 200 kDa (green); nuclei labeled with To-Pro-3 (blue). Surface preparation view (A) and (a) Z-plane image of the cochlea from the control group. Note dense network of nerve fibers, mostly type I auditory nerve fibers, adjacent to the row of inner hair cells (IHC). Note thick fascicles of nerve fibers, mostly type II auditory nerve fibers, projecting our radially towards the outer hair cells (OHC). Surface preparation view (B) and z-plane image of the cochlea from a rat in the 4 mg/kg TMT group. Notes reduced nerve fibers adjacent to the IHC and reduced numbers of fibers projecting radially towards the OHC (arrowheads). Surface preparation (C) and z-plane (c) image from the cochlea of a rat in the 8 mg/kg TMT group. Note diminished nerve fiber labeling near the IHC, the reduction in the number of radial nerve fibers and loss of OHC nuclei (asterisks).

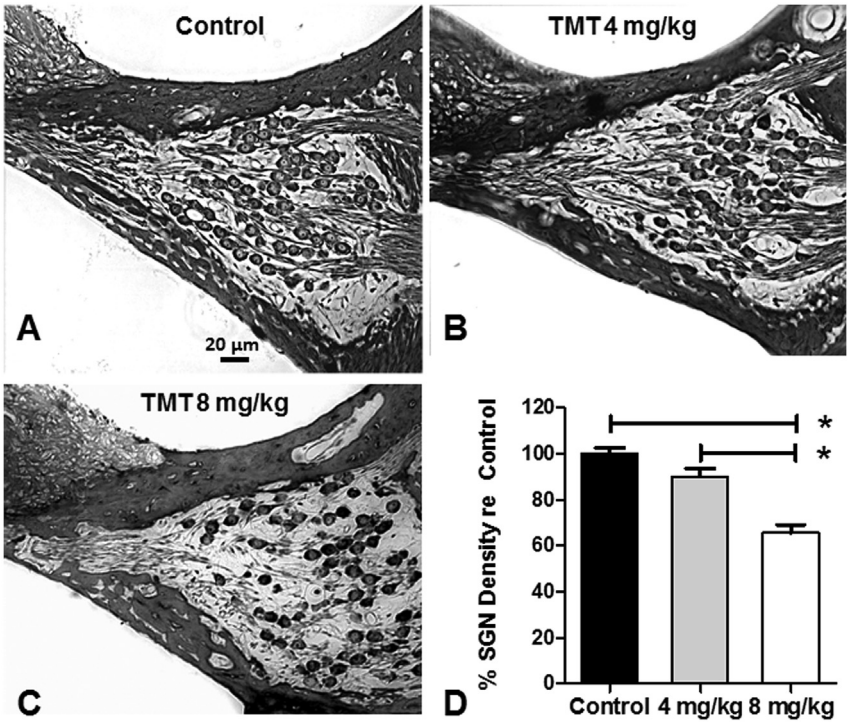

Fig. 4. Loss of spiral ganglion neurons (SGN) at 7 d post-TMT treatment. (A–C) Representative images (200X) of Rosenthal's canal taken from the basal turn of the cochlea from a Control rat and rats treated with 4 mg/kg or 8 mg/kg TMT. (D) Histogram showing the mean (+/− SEM) percent reduction in SGNs in the hook region of the cochlea in the 4 mg/kg (n = 5) and 8 mg/kg (n = 6) TMT groups relative to the Control group (n = 5). There were significantly few SGNs in the 8 mg/kg group compared to the control group and the 4 mg/kg group (*$p < 0.05$).

shown in Fig. 4D, the mean (+/− SEM) SGN density in the 8 mg/kg TMT group was significantly lower than the control group and the 4 mg/kg TMT group (one-way ANOVA, $F = 29.41$, 2, 15 DF, $p < 0.0001$, Newman–Keuls post-hoc comparison, $p < 0.05$).

To gain insights into the mechanism of SGN degeneration, the cochleae were immunolabeled with neurofilament 200 kDa to label the nerve fibers and To-Pro3, a nuclear stain. SGNs from the basal turn of a typical control cochlea (Fig. 5A) had large round soma, cytoplasm heavily labeled with neurofilament (green) and a large, oval-shaped nucleus in the center of the soma. The ANFs labeled with neurofilament appeared as thick fascicles (Fig. 5A). In contrast, the soma of many SGNs in the 4 mg/kg TMT group appeared shrunken and distorted and the nucleus was often condensed and fragmented, morphological features of cells undergoing apoptosis (arrowhead, Fig 5B). Similar morphological changes were observed in the SGNs in the 8 mg/kg TMT group, but the changes were more prevalent and pronounced (Fig. 5C). In addition, most of the neurites in 8 mg/kg TMT group were missing and the neurofilament labeling of the cytoplasm tended to be less intense and less uniform than that seen in controls and in the 4 mg/kg TMT group.

4. Discussion

TMT is widely used for production of plastics in the chemical industry and is an established occupational and environmental health hazard (Borghi and Porte, 2002; Geloso et al., 2011). The first two TMT poisoning cases were reported in 1978 and by 2010 there were more than 1849 cases and 23 deaths recorded from TMT intoxication (Tang et al., 2010). TMT is a potent neurotoxin that mainly damage neurons in CNS (Trabucco et al., 2009). Human TMT cases develop a “limbic-cerebellar syndrome”; the clinical features include hearing loss, disorientation, amnesia, aggressiveness, disturbed sexual behavior, complex partial and tonic-clonic seizures, ataxia and mild sensory neuropathy (Besser et al., 1987). Because of the obvious neurobehavioral changes, most research related to TMT has focused on damage to the CNS with little attention to other less obvious conditions such as hearing impairment (Ruppert et al., 1984; Besser et al., 1987). A limited number of studies have characterized some aspects of TMT ototoxicity (Young and Fechter, 1986; Crofton et al., 1990), but a complete understanding of the functional and structural changes associated with different doses of TMT is lacking.

Our results show that a single 4 mg/kg dose of TMT did not lead to OHC or IHC loss. However, the 4 mg/kg dose of TMT caused a moderate CAP threshold shift at 7 d post-treatment, but CAP thresholds had recovered to pre-treatment values by 28 d post-treatment. Despite the lack of damage to IHCs or OHC and lack of permanent CAP threshold shift, the 4 mg/kg dose of TMT greatly reduced the number of cochlear nerve fibers at 7 d post-treatment, especially the fibers innervating the IHCs, which are predominantly type I ANFs (Spoendlin, 1981). There are several possible explanations for the temporary increase in CAP thresholds at 7 d post-treatment and complete recovery of CAP thresholds at 28 d post-treatment. One possibility is that the temporary CAP threshold shift at 7 d post-treatment is due to transient damage to the ANFs followed by the subsequent repair of the type I ANF terminals that make synaptic contacts with the IHCs (Pujol and Puel, 1999; Wang and Green, 2011). Thus, the repair or regeneration of the type I ANFs and their synaptic connections with IHCs may contribute to recovery of hearing sensitivity. To test this hypothesis, additional, in depth morphological studies are needed to determine if ANFs can regenerate after TMT treatment. On the other hand, the small loss of SGNs after the 4 mg/kg dose of TMT and the large loss following 8 mg/kg of TMT indicate that TMT is highly neurotoxic and that the ANFs and SGNs are the most vulnerable structures to ototraumatic insults. This interpretation is consistent with recent studies showing that the low and medium spontaneous rate ANFs are the most susceptible to noise-induced hearing loss (Kujawa and Liberman, 2009; Lin et al., 2011). Moreover, selective destruction of low and medium spontaneous rate ANFs seems to have little effect on CAP threshold. Thus, the complete recovery of CAP thresholds after 4 mg/kg TMT treatment does not necessarily mean that there is absence of cochlear pathology. Indeed, there is evidence of moderate ANF and SGN damage even after the 4 mg/kg TMT treatment

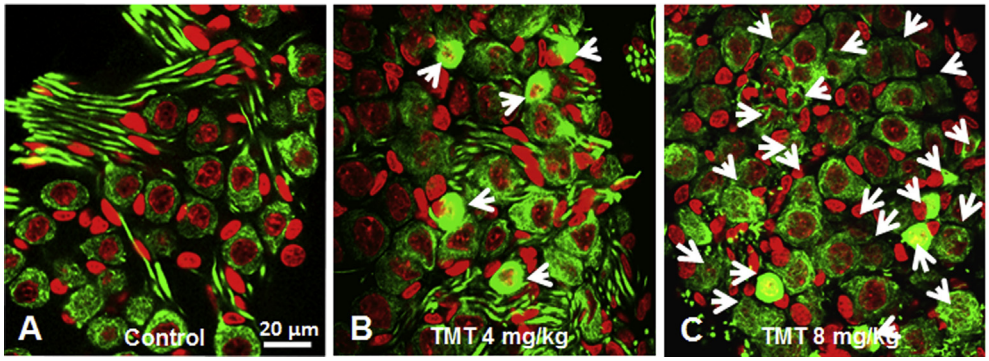

Fig. 5. Representative confocal images showing spiral ganglion neurons (SGNs) in the basal turn of the cochlea 7 d post-treatment. (A) Controls. (B) 4 mg/kg TMT group and (C) 8 mg/kg TMT group. Note SGN with shrunken soma and condensed nuclei (arrowheads). Specimens labeled with an antibody against neurofilament 200 kDa (green); nuclei labeled with To-Pro-3 (red).

(Figs. 4,5). If the TMT were to selectively damage the high-threshold ANFs with low and medium spontaneous rates, this would be expected to reduce the suprathreshold amplitude of the CAP, but have little effect on CAP threshold. In current study, we found that CAP amplitude at 80 dB (SPL) were significantly decreased at all frequencies 28 days post-TMT in the 4 mg/kg and 8 mg/kg groups (Fig. 1C, D). This indicate that although CAP thresholds were restored to near normal levels at all frequencies except 32 kHz in 8 mg/kg group 28, the CAP amplitudes were diminished at all frequencies which likely reflects a prolonged dysfunction in the auditory nerve fibers. The delayed latencies of CAP at 32 kHz were associated with a threshold shift in 8 mg/kg group (Fig. 1F). The increase in latency is likely due to the threshold shift and damage to the ANFs and SGNs. It is noteworthy that CAP thresholds at 4, 8, 16 kHz were completely recovered 28 days post-TMT. However, the latencies at 4, 8, 16 kHz were still prolonged (Fig. 1F). This suggests a dysfunction of auditory nerve fibers consistent with the CAP amplitude reduction (Fig. 1C,D). In any case, our results suggest that low-dose TMT preferentially damages the ANFs beneath the IHCs suggesting that type I ANF may be the most susceptible structures. This result is consistent with previous physiological studies demonstrating that TMT initially disrupts cochlear CAP function while more severe damage depresses the CM potential generated by the OHCs (Fechter et al., 1992).

Based on our in vitro study, TMT preferentially damaged ANF and SGNs, but had no effect to cochlear sensory hair cells. In addition, TMT-induced damage to SGN was always associated with nuclear shrinkage, condensation, or fragmentation, neuroanatomical features of apoptosis (Yu et al., 2015). These findings are very similar to the damage patterns in current *in vivo* study, which may suggest that the neurotoxic effects of TMT are more severe than its toxic effects to sensory hair cells in the inner ear.

At the higher 8 mg/kg dose, TMT caused significant loss of cochlear hair cells, nerve fibers and SGNs. TMT-induced hair cell loss was greatest near the base of the cochlea and OHC loss was more severe than IHC loss. This pattern of damage is similar to that seen with aminoglycoside antibiotics (Forge and Schacht, 2000). However, aminoglycoside antibiotics such as gentamycin and neomycin mainly damage hair cells, but have limited effect on SGNs and nerve fibers (Ding and Salvi, 2005). Also with the 8 mg/kg dose of TMT, neural damage was most severe at the base of the cochlea consistent with the pattern of hair cell loss. SGN loss was observed mainly in the hook region of cochlea where 40–50% of the SGNs were missing. These results indicate that TMT initially damages ANFs and SGNs in the base of the cochlea, but as the dose increases sensory cell loss begins to occur with OHCs being more vulnerable than IHCs.

While we did not explore the mechanisms of TMT-induced damage in detail, confocal microscopy revealed considerable nuclear condensation and soma shrinkage in SGNs, morphological hallmarks of apoptosis. These results are consistent with previous in vitro findings showing TMT-induced SGN damage occurs by apoptosis as reflected by caspase-3 activation (Yu et al., 2015). Studies with neural cell lines and primary cultures suggest that TMT-induced apoptosis is associated with glutamate excitotoxicity, oxidative stress, intracellular calcium overload, and mitochondrial damage (Jenkins and Barone, 2004; Piacentini et al., 2008; Geloso et al., 2011). Given that TMT-induced CAP dysfunction is prevented by antioxidants (Clerici, 1996), it seems likely that reactive oxygen species (ROS) play a major role in TMT-induced SGN damage. Since glutamate is the putative neurotransmitter at the synapse between IHC and type I SGN, TMT-induced excitotoxicity may account for the massive degeneration of nerve fiber terminals below the IHC (Pujol and Puel, 1999).

In summary, our results suggest the synapse between the IHC and type I SGNs may be the most susceptible to TMT-induced cochlear damage. TMT damage is dose and location dependent. As the dose of TMT increases, damage spreads to the OHCs and IHCs in the base of the cochlea. TMT-induced cell death is likely occurs by apoptosis; however, the exact mechanisms by which this occurs will require further study.

Conflict of interest

The authors declare that there are no conflicts of interest.

Acknowledgments

This research was supported in part by grants from the National Institute for Occupational Safety and Health (R01OH010235), the National Nature Science Foundation of China (No. 81170912) and the Major State Basic Research Development Program of China (No. 2014CB943003).

References

Bencko, V., Rames, J., Fabianova, E., Pesek, J., Jakubis, M., 2009. Ecological and human health risk aspects of burning arsenic-rich coal. Environ. Geochem. Health 31 (1), 239–243.

Besser, R., Kramer, G., Thumler, R., Bohl, J., Gutmann, L., Hopf, H.C., 1987. Acute trimethyltin limbic-cerebellar syndrome. Neurology 37, 945–950.

Borghi, V., Porte, C., 2002. Organotin pollution in deep-sea fish from the northwestern mediterranean. Environ. Sci. Technol. 36, 4224–4228.

Clerici, W.J., 1996. Effects of superoxide dismutase and U74389G on acute trimethyltin-induced cochlear dysfunction. Toxicol. Appl. Pharmacol. 136, 236–242.

Clerici, W.J., Ross Jr., B., Fechter, L.D., 1991. Acute ototoxicity of trialkyltins in the Guinea pig. Toxicol. Appl. Pharmacol. 109, 547–556.

Crofton, K.M., Dean, K.F., Menache, M.G., Janssen, R., 1990. Trimethyltin effects on auditory function and cochlear morphology. Toxicol. Appl. Pharmacol. 105, 123–132.

Ding, D., Allman, A., Yin, S., Sun, H., Salvi, R.J., 2011a. Cisplatin Ototoxicity, vol. 2. Nova Science Publishers, Inc, pp. 39–63.

Ding, D., Allman, B.L., Salvi, R., 2012a. Review: ototoxic characteristics of platinum antitumor drugs. Anat. Rec. Hob. 295, 1851–1867.

Ding, D., He, J., Allman, B.L., Yu, D., Jiang, H., Seigel, G.M., Salvi, R.J., 2011b. Cisplatin ototoxicity in rat cochlear organotypic cultures. Hear Res. 282, 196–203.

Ding, D., Jiang, H., Fu, Y., Li, Y., Salvi, R., 2013. Ototoxic model of oxaliplatin and protection from nocitinamide adenine dinucleotide. J. Otol. 8, 22–30.

Ding, D., Jiang, H., Fu, Y., Salvi, R., Someya, S., Tanokura, M., 2012b. Ototoxic effects of carboplatin in cochlear organotypic cultures in chinchillas and rats. J. Otol. 7, 92−101.

Ding, D., Jiang, H., Wang, P., Salvi, R., 2007. Cell death after co-administration of cisplatin and ethacrynic acid. Hear Res. 226, 129−139.

Ding, D., Roth, J., Salvi, R., 2011c. Manganese is toxic to spiral ganglion neurons and hair cells in vitro. Neurotoxicology 32, 233−241.

Ding, D., Salvi, R., 2005. Review of cellular changes in the cochlea due to aminoglycoside antibiotics. Volta. Rev. 105, 407−438.

Ding, D., Wang, P., Jiang, H., Coling, D., Salvi, R., 2009. Gene expression in cisplatin ototoxicity and protection with p53 inhibitor. J. Otol. 4, 15−24.

Ding, D.L., Wang, J., Salvi, R., Henderson, D., Hu, B.H., McFadden, S.L., Mueller, M., 1999. Selective loss of inner hair cells and type-I ganglion neurons in carboplatin-treated chinchillas. Mechanisms of damage and protection. Ann. N. Y. Acad. Sci. 884, 152−170.

Dyer, R.S., Walsh, T.J., Wonderlin, W.F., Bercegeay, M., 1982. The trimethyltin syndrome in rats. Neurobehav. Toxicol. Teratol. 4, 127−133.

Fechter, L.D., Clerici, W.J., Yao, L., Hoeffding, V., 1992. Rapid disruption of cochlear function and structure by trimethyltin in the Guinea pig. Hear Res. 58, 166−174.

Fechter, L.D., Liu, Y., 1995. Elevation of intracellular calcium levels in spiral ganglion cells by trimethyltin. Hear. Res. 91, 101−109.

Fechter, L.D., Young, J.S., Nuttall, A.L., 1986. Trimethyltin ototoxicity: evidence for a cochlear site of injury. Hear Res. 23, 275−282.

Forge, A., Schacht, J., 2000. Aminoglycoside antibiotics. Audiol. Neurootol. 5, 3−22.

Geloso, M.C., Corvino, V., Michetti, F., 2011. Trimethyltin-induced hippocampal degeneration as a tool to investigate neurodegenerative processes. Neurochem. Int. 58, 729−738.

He, J., Ding, D., Yu, D., Jiang, H., Yin, S., Salvi, R., 2011. Modulation of copper transporters in protection against cisplatin-induced cochlear hair cell damage. J. Otol. 6, 53−61.

Hoshino, A.C., Ferreira, H.P., Malm, O., Carvallo, R.M., Camara, V.M., 2012. A systematic review of mercury ototoxicity. Cad. Saude Publica 28, 1239−1248.

Ikeda, T., Takahashi, K., Kabata, T., Sakagoshi, D., Tomita, K., Yamada, M., 2010. Polyneuropathy caused by cobalt-chromium metallosis after total hip replacement. Muscle Nerve 42, 140−143.

Ishikura, N., Tsunashima, K., Watanabe, K., Nishimura, T., Minabe, Y., Kato, N., 2002. Neuropeptide Y and somatostatin participate differently in the seizure-generating mechanisms following trimethyltin-induced hippocampal damage. Neurosci. Res. 44, 237−248.

Jarup, L., 2003. Hazards of heavy metal contamination. Br. Med. Bull. 68, 167−182.

Jenkins, S.M., Barone, S., 2004. The neurotoxicant trimethyltin induces apoptosis via caspase activation, p38 protein kinase, and oxidative stress in PC12 cells. Toxicol. Lett. 147, 63−72.

Koczyk, D., 1996. How does trimethyltin affect the brain: facts and hypotheses. Acta Neurobiol. Exp. (Wars) 56, 587−596.

Kujawa, S.G., Liberman, M.C., 2009. Adding insult to injury: cochlear nerve degeneration after “temporary” noise-induced hearing loss. J. Neurosci. 29, 14077−14085.

Li, P., Ding, D., Salvi, R., Roth, J.A., 2015. Cobalt-induced ototoxicity in rat postnatal cochlear organotypic cultures. Neurotox. Res. 28, 209−221.

Li, Y., Ding, D., Jiang, H., Fu, Y., Salvi, R., 2011. Co-administration of cisplatin and furosemide causes rapid and massive loss of cochlear hair cells in mice. Neurotox. Res. 20, 307−319.

Lin, H.W., Furman, A.C., Kujawa, S.G., Liberman, M.C., 2011. Primary neural degeneration in the Guinea pig cochlea after reversible noise-induced threshold shift. J. Assoc. Res. Otolaryngology JARO 12, 605−616.

Liu, H., Ding, D., Sun, H., Jiang, H., Wu, X., Roth, J.A., Salvi, R., 2014. Cadmium-induced ototoxicity in rat cochlear organotypic cultures. Neurotox. Res. 26, 179−189.

Nilsberth, C., Kostyszyn, B., Luthman, J., 2002. Changes in APP, PS1 and other factors related to Alzheimer's disease pathophysiology after trimethyltin-induced brain lesion in the rat. Neurotox. Res. 4, 625−636.

Piacentini, R., Gangitano, C., Ceccariglia, S., Del Fa, A., Azzena, G.B., Michetti, F., Grassi, C., 2008. Dysregulation of intracellular calcium homeostasis is responsible for neuronal death in an experimental model of selective hippocampal degeneration induced by trimethyltin. J. Neurochem. 105, 2109−2121.

Prasher, D., 2009. Heavy metals and noise exposure: health effects. Noise Health 11, 141−144.

Pujol, R., Puel, J.L., 1999. Excitotoxicity, synaptic repair, and functional recovery in the mammalian cochlea: a review of recent findings. Ann. N. Y. Acad. Sci. 884, 249−254.

Ruppert, P.H., Dean, K.F., Reiter, L.W., 1984. Trimethyltin disrupts acoustic startle responding in adult rats. Toxicol. Lett. 22, 33−38.

Shargorodsky, J., Curhan, S.G., Henderson, E., Eavey, R., Curhan, G.C., 2011. Heavy metals exposure and hearing loss in US adolescents. Arch. Otolaryngol. Head. Neck Surg. 137, 1183−1189.

Spoendlin, H., 1978. The afferent innervation of the cochlea. In: Naunton, R.F., Fernandez, C. (Eds.), Evoked Electrical Activity in the Auditory Nervous System, vol. 272. Academic Press, New York, pp. 21−41.

Spoendlin, H., 1981. Autonomic innervation of the inner ear. Adv. Oto-Rhino-Laryngology 27, 1−13.

Tang, X., Yang, X., Lai, G., Guo, J., Xia, L., Wu, B., Xie, Y., Huang, M., Chen, J., Ruan, X., Sui, G., Ge, Y., Zuo, W., Zhao, N., Zhu, G., Zhang, J., Li, L., Zhou, W., 2010. Mechanism underlying hypokalemia induced by trimethyltin chloride: inhibition of H^+/K^+-ATPase in renal intercalated cells. Toxicology 271, 45−50.

Trabucco, A., Di Pietro, P., Nori, S.L., Fulceri, F., Fumagalli, L., Paparelli, A., Fornai, F., 2009. Methylated tin toxicity a reappraisal using rodents models. Arch. Ital. Biol. 147, 141−153.

Wang, J., Ding, D., Salvi, R.J., 2003. Carboplatin-induced early cochlear lesion in chinchillas. Hear Res. 181, 65−72.

Wang, L., Ding, D., Salvi, R., Roth, J.A., 2014. Nicotinamide adenine dinucleotide prevents neuroaxonal degeneration induced by manganese in cochlear organotypic cultures. Neurotoxicology 40, 65−74.

Wang, Q., Green, S.H., 2011. Functional role of neurotrophin-3 in synapse regeneration by spiral ganglion neurons on inner hair cells after excitotoxic trauma in vitro. J. Neurosci. 31, 7938−7949.

Warr, W.B., 1992. Organization of olivocochlear efferent systems in mammals. In: Webster, D.B., et al. (Eds.), The Mammalian Auditory Pathway: Neuroanatomy. Springer Verlag, New York, pp. 410−448.

White, J.S., Warr, W.B., 1983. The dual origins of the olivocochlear bundle in the albino rat. J. Comp. Neurol. 219, 203−214.

Wu, X., Ding, D., Salvi, R., 2011. Lead neurotoxicity in rat cochlear organotypic cultures. J. Otology 43−50.

Young, J.S., Fechter, L.D., 1986. Trimethyltin exposure produces an unusual form of toxic auditory damage in rats. Toxicol. Appl. Pharmacol. 82, 87−93.

Yu, J., Ding, D., Sun, H., Salvi, R., Roth, J.A., 2015. Neurotoxicity of trimethyltin in rat cochlear organotypic cultures. Neurotox. Res. 28, 43−54.

Yu, J., Ding, D., Wang, F., Jiang, H., Sun, H., Salvi, R., 2014. Pattern of hair cell loss and delayed peripheral neuron degeneration in inner ear by a high-dose intratympanic gentamicin. J. Otol. 9, 126−135.